



# Journal of Applied Sciences

ISSN 1812-5654

**science**  
alert

**ANSI***net*  
an open access publisher  
<http://ansinet.com>

## Prediction of the Concentration of Diethanolamine (DEA) and Methyldiethanolamine (MDEA) Aqueous Solutions by Using Raman Spectroscopy

Muhammad Zubair Shahid, Abdulhalim Shah Maulud and M. Azmi Bustam  
Department of Chemical Engineering, Universiti Teknologi PETRONAS, Bandar Seri Iskandar,  
Tronoh Perak Darul Ridzuan, 31750, Malaysia

**Abstract:** Aqueous solutions of alkanolamines such as DEA and MDEA in different concentrations have been using for many years to remove carbon dioxide from natural gas. The concentration monitoring of amine solution is an important objective to ensure the gas absorption process is properly functioning and optimized. Raman spectroscopy is a suitable quick response technique to predict the composition of aqueous solutions at offline and online situations, because of its weak Raman scattering property for water. In this work, aqueous solutions of DEA and MDEA are prepared over different concentrations and their Raman spectra are recorded in offline situation. Three significant wave numbers for each of DEA (1292.3, 1065, 1465.2  $\text{cm}^{-1}$ ) and MDEA (338, 745.4, 1458.5  $\text{cm}^{-1}$ ) were identified and found that 1465.2 and 1458.5  $\text{cm}^{-1}$  respectively are the best linear fit.

**Key words:** Raman spectroscopy, aqueous amines, quantitative prediction

### INTRODUCTION

Natural gas have been using as a source of energy and raw material for the production of many synthetic products. However, this natural gas may contain  $\text{CO}_2$  which is a concern because it is a greenhouse gas. The carbon dioxide gas is also released from power plants, transportation sources and other human activities which are the cause of increasing global warming, while world will continue to rely on fossil fuels for the generation of energy probably for next 20-30 years (Wong and Bioletti, 2002). Therefore carbon dioxide capturing has been a pressing issue since many years. One of the most commonly used process for  $\text{CO}_2$  capturing is using alkanolamine which has been considered as the best approach to be used for the post combustion removal of  $\text{CO}_2$  in coal fired power plants, which contributes about 30% of  $\text{CO}_2$  emissions (Rochelle, 2009). Many types of alkanolamines have been used for  $\text{CO}_2$  capturing such as, Monoethanolamine (MEA), Diethanolamine (DEA), Methyldiethanolamine (MDEA), Di-2-propanolamine (DIPA) and sterically hindered amines such as 2-amino-2-methyl-1-propanol (AMP) (Alie *et al.*, 2006; Idem *et al.*, 2006; Zhang *et al.*, 2008).

In the gas capturing process, amine solution is allowed to enter into the absorption section where it absorbs  $\text{CO}_2$  at low temperature and high pressure and for the regeneration of amine solution, amine solution transfers into the stripping section where  $\text{CO}_2$  strips out with water vapors at high temperature and low pressure

(Yeh *et al.*, 2001; Rochelle, 2009). However, in this complete cycle of  $\text{CO}_2$  capturing and the regeneration of amine solution, the concentration of solution changes due to chemical loss and water dilutions. While in long term amine solutions are also degraded and it produces various undesirable products, such as N-formylethanolamine ( $\text{C}_3\text{N}_7\text{NO}_2$ ), 1-(2-hydroxyethyl)-2-imidazolidinone ( $\text{C}_5\text{H}_{10}\text{N}_2\text{O}_2$ ), acetic acid ( $\text{C}_2\text{H}_4\text{O}_2$ ) and many others (Islam *et al.*, 2011). The variation in amine solution concentration and degraded products can cause corrosion of equipment and also adversely affect the gas loading capacity and their gas capturing rate, so it disturbs the economy of the reaction (Wong and Bioletti, 2002; Huttenhuis *et al.*, 2007; Islam *et al.*, 2011). Therefore, in order to keep the system economical and optimized, it is required to develop a fast online monitoring system that able to measure the concentration of alkanolamine in its aqueous solution, so that variations in the amine solution concentration during capturing and regeneration process can be monitored and controlled.

For the online and fast monitoring of chemical reactions, many spectroscopic techniques have been used such as, to measure the concentration of reactants or products or molecular weights or to identify the product quality and kinetics in the polymerization reactions (Scherzer and Decker, 1999; Bauer *et al.*, 2000; Reis *et al.*, 2005). The selection of spectroscopic techniques to monitor chemical reaction depends upon the nature of reactants, products and the medium

(Ferraro *et al.*, 1994). In the present case, we are monitoring aqueous amine solutions and for this purpose, Raman spectroscopy is selected because of its weak sensitivity to the water molecules (Ferraro *et al.*, 1994; Reis *et al.*, 2005), so it does not disturb the spectra to much extent. As compared to InfraRed (IR) is very sensitive to water and the presence of water may cause problem for accurate alkanolamine aqueous solution quantification analysis.

### MATERIALS AND METHODS

The experimental setup is shown in Fig. 1. The portable Raman spectrometry apparatus manufactured by StellarNet was used. The laser source had wavelength of 785 nm and power of 499 mW while its beam diameter at the exit of fiber bulkhead was 105  $\mu\text{m}$ . The spectrometer was specially configured for Raman spectrums to produce optical resolution of 4  $\text{cm}^{-1}$  and signal to noise ratio of 1000:1. The software SpectraWiz was used to capture the spectra. In the experimentation process, the laser beam through optical fiber was reached to the sample placed in the optical fiber probe box and scattered back to spectrometer where it detected the Raman Effect and produced the respective Raman spectrum on the computer. For the settings of spectrum preprocessing, the boxcar smoothing was kept as 3, which means the total 17 pixels arrangement and the number of scans to average ratio as 1 while the integration time for the spectrum was fixed at 10 seconds. DEA and MDEA were purchased from Merck with purity of 99% and were used for making their solutions into ten different concentrations by weight in distilled water. The weight was measured up to 4 decimal digits. Each of the solution in the vial was placed in the probe box and five spectrums were captured for each of the concentration. In all of the intensities, the maximum peak was normalized to the scale of hundred for the conveniency. The average generated normalized intensities of selected Raman Peaks are fitted against the known concentrations with a linear fit and calibration models are produced. In order to validate the calibration models, validation data set was made by randomly selecting the three concentrations. A linear fit between the predicted and actual concentration values was then performed on the validation. The performance was reported in terms of  $R^2$  and mean square error (MSE) values, where MSE is the average of the square of the difference between actual and predicted concentrations of the solutions.

### RESULTS AND DISCUSSION

Figures 2 and 3 show the selected spectra of DEA and MDEA aqueous solutions respectively, of different

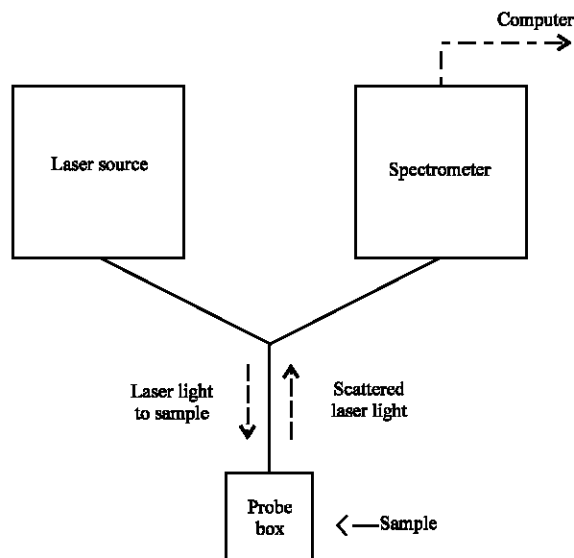


Fig. 1: Experimentation schematic diagram

concentrations. It can be seen that all the peaks height are decreasing as the concentration of DEA and MDEA reducing. This is because of Raman spectra of water is comparatively weak and all the peaks are representing the alkanolamines. Therefore, as the alkanolamine concentration decreasing, the strength of scattered laser is decreasing and peak heights are lessening. For each of DEA and MDEA, three dominant peaks are identified and selected which are shown in Fig. 2 as (1065.7, 1292.3 and 1465.2  $\text{cm}^{-1}$ ) and in Fig. 3 (338.7, 745.4 and 1458.5  $\text{cm}^{-1}$ ), respectively.

The normalized intensity or peak height of these peaks are used to calibrate the solutions concentrations by fitting with a linear relationship. The average intensities along with their standard deviation are shown in the Table 1 and Table 2. The linear fittings with the standard deviation error bars are depicted in the Fig. 4(a-f) and Fig. 5(a-f) for both DEA and MDEA aqueous solutions respectively. It can be seen that both the validation data and calibration data points are appropriately defined by the linear relationship.

In Table 3 and 4, all the fitted data points with their  $R^2$  values and their MSE are shown. In the case of DEA, the  $R^2$  value for all the peaks are greater than 0.960 and the maximum value is 0.990 for the calibration fitting of peak 1465.2  $\text{cm}^{-1}$ . For a validation set, the fitting is performed between the actual and predicted concentration of solution. Peak 1465.2  $\text{cm}^{-1}$  shows the best  $R^2$  (0.978) in the validation set. In addition, the mean square error is also the least for this peak which is 0.00071 and 0.00470 for the calibration and validation sets, respectively. This concludes that peak 1465.2  $\text{cm}^{-1}$  produces the best prediction among the three peaks. While in the case of

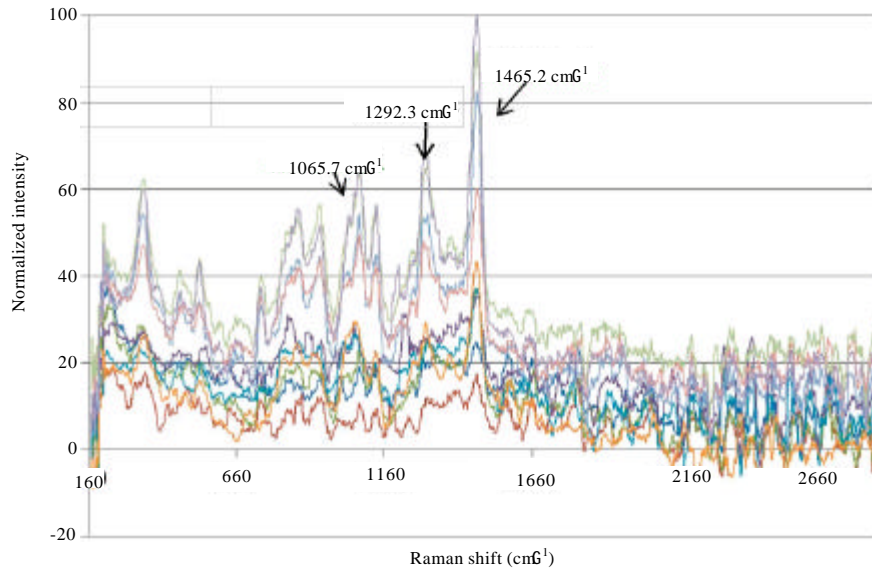


Fig. 2: DEA (aqueous solutions) spectra

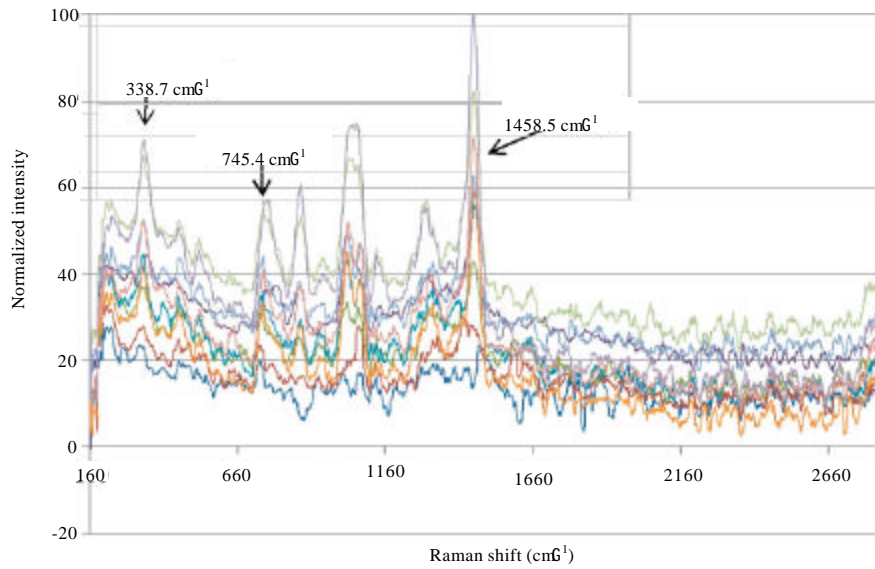


Fig. 3: MDEA (aqueous solutions) spectra

Table 1: DEA Intensities of selected wave numbers with their standard deviation (SD)

| Mass fraction | 1065.7 cm <sup>-1</sup> |        | 1292.3 cm <sup>-1</sup> |        | 1465.2 cm <sup>-1</sup> |        |
|---------------|-------------------------|--------|-------------------------|--------|-------------------------|--------|
|               | Average                 | SD     | Average                 | SD     | Average                 | SD     |
| 0.099*        | 14.496                  | 5.450  | 16.805                  | 4.730  | 13.927                  | 5.238  |
| 0.201         | 13.541                  | 6.144  | 15.251                  | 7.078  | 16.136                  | 7.034  |
| 0.300         | 21.145                  | 9.193  | 23.212                  | 9.396  | 24.079                  | 8.885  |
| 0.401         | 28.339                  | 6.354  | 29.561                  | 6.605  | 27.045                  | 3.705  |
| 0.491         | 28.456                  | 9.322  | 29.950                  | 9.905  | 37.193                  | 7.903  |
| 0.602*        | 44.377                  | 21.755 | 45.725                  | 20.989 | 45.307                  | 16.082 |
| 0.699         | 57.465                  | 21.784 | 57.242                  | 22.137 | 54.147                  | 22.591 |
| 0.788         | 69.315                  | 13.605 | 69.123                  | 13.725 | 66.312                  | 17.099 |
| 0.907*        | 79.304                  | 12.963 | 80.162                  | 13.649 | 77.636                  | 16.738 |
| 1.000         | 82.904                  | 12.556 | 86.739                  | 15.092 | 83.064                  | 14.588 |

\*Validation data points

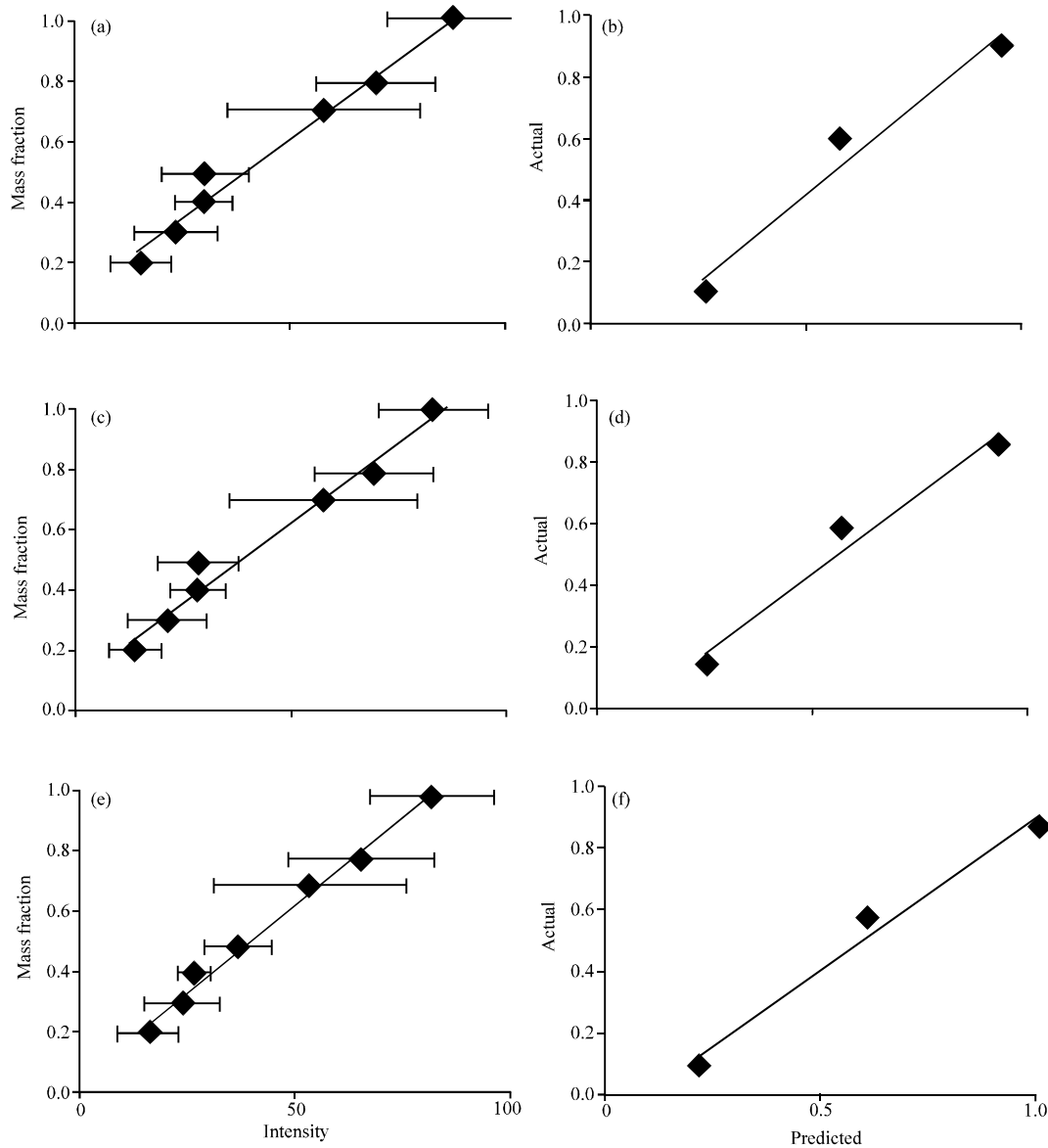


Fig. 4(a-f): DEA calibration and validation results, (a) Peak 1065.7 (calibration), (b) Peak 1065.7 (validation), (c) Peak 1465.2 (calibration), (d) Peak 1465.2 (validation), (e) Peak 1292.3 (calibration) and (f) Peak 1292.3 (validation)

Table 2: MDEA Intensities of selected wave numbers with their standard deviation (SD)

| Mass fraction | 1065.7 cm <sup>-1</sup> |        | 1292.3 cm <sup>-1</sup> |        | 1465.2 cm <sup>-1</sup> |        |
|---------------|-------------------------|--------|-------------------------|--------|-------------------------|--------|
|               | Average                 | SD     | Average                 | SD     | Average                 | SD     |
| 0.110         | 41.010                  | 12.943 | 44.808                  | 15.301 | 21.103                  | 7.871  |
| 0.200*        | 44.399                  | 5.77   | 43.371                  | 6.690  | 29.725                  | 7.779  |
| 0.313         | 51.419                  | 6.818  | 55.102                  | 6.528  | 37.786                  | 3.764  |
| 0.406         | 37.593                  | 14.485 | 36.919                  | 16.853 | 41.547                  | 10.546 |
| 0.489         | 52.032                  | 6.734  | 52.900                  | 6.496  | 46.527                  | 5.892  |
| 0.601*        | 54.360                  | 6.080  | 53.926                  | 6.774  | 51.913                  | 10.627 |
| 0.708         | 63.542                  | 13.472 | 63.577                  | 15.362 | 54.538                  | 10.162 |
| 0.804         | 66.273                  | 15.174 | 68.212                  | 15.848 | 61.512                  | 10.243 |
| 0.895         | 72.734                  | 13.983 | 72.722                  | 16.474 | 69.651                  | 14.815 |
| 1.000*        | 82.638                  | 10.951 | 83.129                  | 10.878 | 71.280                  | 18.817 |

\*Validation data points

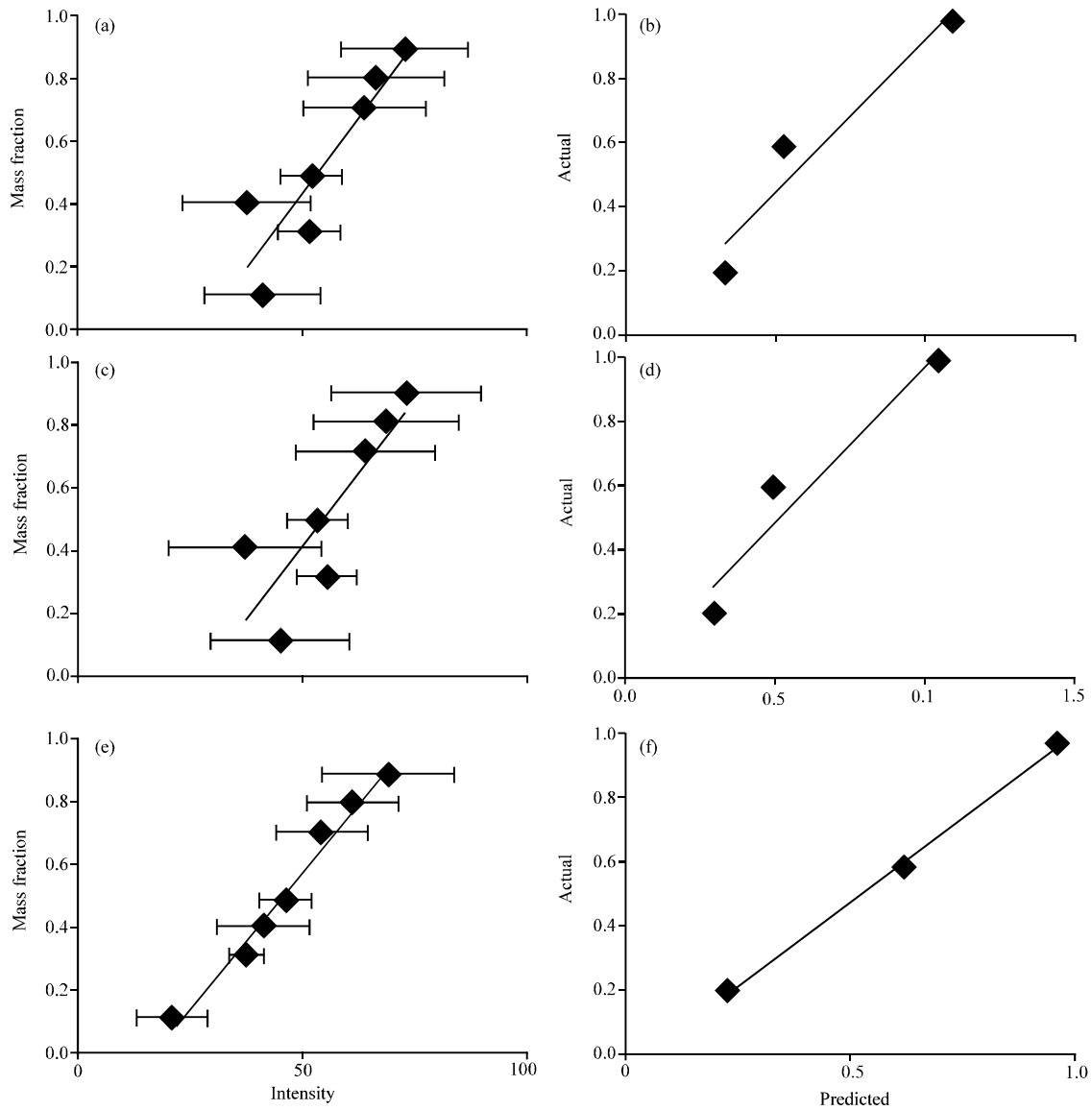


Fig. 5(a-f): MDEA calibration and validation result, DEA calibration and validation results, (a) Peak 1065.7 (calibration), (b) Peak 1065.7 (validation), (c) Peak 1465.2 (calibration), (d) Peak 1465.2 (validation), (e) Peak 1292.3 (calibration) and (f) Peak 1292.3 (validation)

Table 3: DEA R<sup>2</sup> and mean square error (MSE)

| Peak   | Calibration    |         | Validation     |         |
|--------|----------------|---------|----------------|---------|
|        | R <sup>2</sup> | MSE     | R <sup>2</sup> | MSE     |
| 1065.7 | 0.974          | 0.00186 | 0.966          | 0.00854 |
| 1292.3 | 0.976          | 0.00478 | 0.964          | 0.00954 |
| 1465.2 | 0.990          | 0.00071 | 0.978          | 0.00470 |

Table 4: MDEA R<sup>2</sup> and mean square error (MSE)

| Peak   | Calibration    |        | Validation     |        |
|--------|----------------|--------|----------------|--------|
|        | R <sup>2</sup> | MSE    | R <sup>2</sup> | MSE    |
| 338    | 0.806          | 0.0144 | 0.928          | 0.0089 |
| 745    | 0.699          | 0.0207 | 0.931          | 0.0074 |
| 1458.5 | 0.981          | 0.0013 | 0.999          | 0.0011 |

MDEA there is more variation in the error. The best peak is  $1458.5\text{ cm}^{-1}$  having the  $R^2$  value of 0.981 and 0.999 for the calibration and validation sets, respectively. Similarly, peak  $1458.5\text{ cm}^{-1}$  produces the least MSE for the calibration (0.0013) and validation (0.0011) sets, respectively. This concludes that peak  $1458.5\text{ cm}^{-1}$  produces the best prediction among the three peaks.

### CONCLUSION

In this work Raman spectroscopy is shown to be a feasible technique to predict the concentration of DEA and MDEA in their aqueous solutions. The best Raman spectra peak for the DEA is  $1465.2\text{ cm}^{-1}$  while for MDEA is  $1458.5\text{ cm}^{-1}$  to predict the concentration with least error values.

### ACKNOWLEDGMENT

The authors wish to acknowledge the financial support provided by Malaysia Ministry of Higher Education to undertake this research work through FRGS grant.

### REFERENCES

- Alie, C., P. Douglas and E. Croiset, 2006. Simulation and optimization of a coal-fired power plant with integrated  $\text{CO}_2$  capture using MEA scrubbing. Proceedings of the 8th International Conference on Greenhouse Gas Control Technologies, June 19-22, 2006, Trondheim, Norway, pp: 1-7.
- Bauer, C., B. Amram, M. Agnely, D. Charmot, J. Sawatzki, N. Dupuy and J.P. Huvenne, 2000. On-line monitoring of a latex emulsion polymerization by fiber-optic FT-Raman spectroscopy. Part I: Calibration. *Applied Spectrosc.*, 54: 528-535.
- Ferraro, J.R., K. Nakamoto and C.W. Brown, 1994. *Introductory Raman Spectroscopy*. 2nd Edn., Elsevier Inc., USA., ISBN-13: 9780122541056.
- Huttenhuis, P.J.G., N.J. Agrawal, J.A. Hogendoorn and G.F. Versteeg, 2007. Gas solubility of  $\text{H}_2\text{S}$  and  $\text{CO}_2$  in aqueous solutions of *N*-methyldiethanolamine. *J. Pet. Sci. Eng.*, 55: 122-134.
- Idem, R., M. Wilson, P. Tontiwachwuthikul, A. Chakma, A. Veawab, A. Aroonwilas and D. Gelowitz, 2006. Pilot plant studies of the  $\text{CO}_2$  capture performance of aqueous MEA and Mixed MEA/MDEA solvents at the university of Regina  $\text{CO}_2$  capture technology development plant and the boundary dam  $\text{CO}_2$  capture demonstration plant. *Ind. Eng. Chem. Res.*, 45: 2414-2420.
- Islam, M.S., R. Yusoff, B.S. Ali, M.N. Islam and M.H. Chakrabarti, 2011. Degradation studies of amines and alkanolamines during sour gas treatment process. *Int. J. Phys. Sci.*, 6: 5883-5896.
- Reis, M.M., M. Uliana, C. Sayer, P.H.H. Araujo and R. Giudici, 2005. Monitoring emulsion homopolymerization reactions using FT-Raman spectroscopy. *Braz. J. Chem. Eng.*, 22: 61-74.
- Rochelle, G.T., 2009. Amine scrubbing for  $\text{CO}_2$  capture. *Science*, 325: 1652-1654.
- Scherzer, T. and A.U. Decker, 1999. Real-time FTIR-ATR spectroscopy to study the kinetics of ultrafast photopolymerization reactions induced by monochromatic UV light. *Vibr. Spectrosc.*, 19: 385-398.
- Wong, S. and R. Bioletti, 2002. Carbon dioxide separation technologies. Alberta Research Council, Canada.
- Yeh, J.T., H.W. Pennline and K.P. Resnik, 2001. Study of  $\text{CO}_2$  absorption and desorption in a packed column. *Energy Fuels*, 15: 274-278.
- Zhang, P., Y. Shi, J. Wei, W. Zhao and Q. Ye, 2008. Regeneration of 2-amino-2-methyl-1-propanol used for carbon dioxide absorption. *J. Environ. Sci.*, 20: 39-44.